ISSN 1674-1056
http://cpb.iphy.ac.cn
http://iopscience.iop.org/cpb
中国物理 B
Chinese Physics
中国物理 Chinese Physics B

Observing the steady-state visual evoked potentials with a compact quad-channel spin exchange relaxation-free magnetometer

Pengcheng Du(杜鹏程), Jianjun Li(李建军), Sijia Yang(杨思嘉), Xutong Wang(王旭桐), Yan Zhuo(卓彦), Fan Wang(王帆), Ruquan Wang(王如泉)

Citation: Chin. Phys. B . 2019, 28(4): 040702. **doi:** 10.1088/1674-1056/28/4/040702
Journal homepage: http://cpb.iphy.ac.cn; http://iopscience.iop.org/cpb

What follows is a list of articles you may be interested in

Magnetic field analysis in a diamond anvil cell for Meissner effect measurement by using the diamond NV^- center

Lin Zhao(赵琳), Donghui Yue(岳冬辉), Cailong Liu(刘才龙), Min Wang(王敏), Yonghao Han(韩永昊), Chunxiao Gao(高春晓)

Chin. Phys. B . 2019, 28(3): 030702. **doi:** 10.1088/1674-1056/28/3/030702

Damage and recovery of fiber Bragg grating under radiation environment

Shi-Zhe Wen(温世喆), Wei-Chen Xiong(熊伟晨), Li-Ping Huang(黄力平), Zhen-Rui Wang(王镇锐), Xing-Bin Zhang(张兴斌), Zhen-Hui He(何振辉)

Chin. Phys. B . 2018, 27(9): 090701. **doi:** 10.1088/1674-1056/27/9/090701

Highly-sensitive NO, NO_2, and NH_3 measurements with an open-multipass cell based on mid-infrared wavelength modulation spectroscopy

Xiang Chen(陈祥), Chen-Guang Yang(杨晨光), Mai Hu(胡迈), Jian-Kang Shen(沈建康), Er-Chao Niu(牛二超), Zhen-Yu Xu(许振宇), Xue-Li Fan(范雪丽), Min Wei(魏敏), Lu Yao(姚路), Ya-Bai He(何亚柏), Jian-Guo Liu(刘建国), Rui-Feng Kan(阚瑞峰)

Chin. Phys. B . 2018, 27(4): 040701. **doi:** 10.1088/1674-1056/27/4/040701

A dual-axis, high-sensitivity atomic magnetometer

Rujie Li(李茹杰), Wei Quan(全伟), Wenfeng Fan(范文峰), Li Xing(邢力), Zhuo Wang(王卓), Yueyang Zhai(翟跃阳), Jiancheng Fang(房建成)

Chin. Phys. B . 2017, 26(12): 120702. **doi:** 10.1088/1674-1056/26/12/120702

Optical sensors based on the NiPc–CoPc composite films deposited by drop casting and under the action of centrifugal force

Noshin Fatima, Muhammad M Ahmed, Khasan S Karimov, Zubair Ahmad, Fahmi Fariq Muhammad

Chin. Phys. B . 2017, 26(6): 060704. **doi:** 10.1088/1674-1056/26/6/060704

Observing the steady-state visual evoked potentials with a compact quad-channel spin exchange relaxation-free magnetometer*

Peng-Cheng Du(杜鹏程)[1,3,†], Jian-Jun Li(李建军)[1,3,†], Si-Jia Yang(杨思嘉)[2,4,6], Xu-Tong Wang(王旭桐)[1], Yan Zhuo(卓彦)[2,4,6], Fan Wang(王帆)[2,4,5,6,‡], and Ru-Quan Wang(王如泉)[1,3,§]

[1] *Institute of Physics, Chinese Academy of Sciences, Beijing* 100190, *China*
[2] *State Key Laboratory of Brain and Cognitive Science, Institute of Biophysics, Chinese Academy of Sciences (CAS), Beijing* 100101, *China*
[3] *School of Physical Sciences, University of Chinese Academy of Sciences, Beijing* 100049, *China*
[4] *CAS Center for Excellence in Brain Science and Intelligence Technology, Beijing* 100101, *China*
[5] *Sino-Danish College, University of Chinese Academy of Sciences, Beijing* 100190, *China*
[6] *University of Chinese Academy of Sciences, Beijing* 100049, *China*

(Received 11 January 2019; revised manuscript received 23 February 2019; published online 19 March 2019)

We observed the steady-state visually evoked potential (SSVEP) from a healthy subject using a compact quad-channel potassium spin exchange relaxation-free (SERF) optically pumped magnetometer (OPM). To this end, 30 s of data were collected, and SSVEP-related magnetic responses with signal intensity ranging from 150 fT to 300 fT were observed for all four channels. The corresponding signal to noise ratio (SNR) was in the range of 3.5–5.5. We then used different channels to operate the sensor as a gradiometer. In the specific case of detecting SSVEP, we noticed that the short channel separation distance led to a strongly diminished gradiometer signal. Although not optimal for the case of SSVEP detection, this set-up can prove to be highly useful for other magnetoencephalography (MEG) paradigms that require good noise cancellation. Considering its compactness, low cost, and good performance, the K-SERF sensor has great potential for biomagnetic field measurements and brain-computer interfaces (BCI).

Keywords: optically pumped magnetometers, steady-state visually evoked potentials, magnetoencephalography

PACS: 07.07.Df, 87.85.Ox, 07.55.Ge, 87.19.le **DOI:** 10.1088/1674-1056/28/4/040702

1. Introduction

Magnetoencephalography (MEG) is a modern neuroimaging technology used for detection of brain-generated magnetic fields with unmatched temporal resolution. It can non-invasively map the magnetic field produced by neuronal currents in the human brain.[1,2] Compared to electroencephalography (EEG), MEG has a higher spatial resolution (about 1 mm), and in contrast to electric current, the magnetic field is not attenuated by skin or skull. Apart from numerous clinical applications,[3–6] MEG is also useful in the field of brain-computer interfacing (BCI),[7–12] where a person's neural activity is directly detected to achieve communication with the external environment.

However, the field intensities observable at the outer layer of the scalp are only in the range of tens of femtotesla (fT).[1] The detection of such extremely weak magnetic fields is a great challenge in terms of sensor technology and suppression of environmental noise. Until recently, the superconducting quantum interference device (SQUID)[13] magnetometers are the mainly sensors used in MEG. However, owing to the cryogenic cooling requirement, it has certain disadvantages, such as high maintenance cost, inflexible sensor array, and reduced MEG signal due to long sensor-head distance.

In the past few decades, spin exchange relaxation-free (SERF)[14–21] optically pumped magnetometers (OPMs) have become a very promising replacement for SQUIDs as sensors for MEG systems. They can work at room temperature without cryogenic cooling, which lowers the cost and shortens the sensor-head distance. The sensor array could be flexible or even made into a wearable device to study brain magnetism during motion,[22] which has sparked great interest in the field of MEG.[23]

OPMs have been previously used to measure magnetic brain responses to non-visual stimulation, like auditory stimulation[24,25] or compound muscle action potentials (CMAP).[26] In this work, we detected the magnetic component of the steady-state visually evoked potential (SSVEP)[27] signals by using a low-cost, portable quad-channel SERF

*Project supported by the National Key Research and Development Program of China (Grant Nos. 2016YFA0300600 and 2016YFA0301500), the Strategic Priority Research Program of Chinese Academy of Sciences (Grant Nos. XDB07030000 and XDBS32000000), the National Natural Science Foundation of China (Grant Nos. 11474347 and 31730039), and the Fund from the Ministry of Science and Technology of China (Grant No. 2015CB351701).

†These authors contributed equally to this work.
‡Corresponding author. E-mail: fanwang@ibp.ac.cn
§Corresponding author. E-mail: ruquanwang@iphy.ac.cn

© 2019 Chinese Physical Society and IOP Publishing Ltd

OPM. Upon exciting the eyes with a visual stimulus at a fixed frequency, the brain generated an SSVEP response at the same frequency and its harmonics, measured in the range of 150 fT–300 fT. The different channels of our OPM achieved a signal to noise ratio (SNR) between 3.5 and 5.5 with 30-s measurement time. In gradiometer configuration, the intrinsic sensitivity was below 10 fT/Hz$^{1/2}$.

2. Experimental setup

The experimental process for obtaining the SSVEP signal is shown in Fig. 1. The subject sat and was asked to look at the picture attentively, which was rendered on the screen using a projector. Black and white squares appeared on the screen interchangeably (see Fig. 2(d)), flickering with a fixed frequency. During the observation of the stimulus, an SSVEP response will appear in the occipital cortex of the human brain (generally in the red area of Fig. 1). The y–z plane of the OPM (shown in Fig. 2(b)) was attached to the scalp area over the occipital cortex (see Fig. 2(a)), which ensures that the sensor detects the magnetic field perpendicular to the scalp. All experimental procedures were performed in a magnetically shielded room (MSR, Vacuumschmelze GmbH & Co. KG, Hanau, Germany, see Fig. 2(d)).

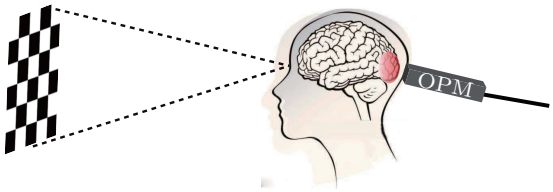


Fig. 1. SSVEP stimulus: black and white squares appearing on the screen interchangeably, flickering at a fixed frequency. The OPM is attached to the scalp area over the occipital cortex (red area).

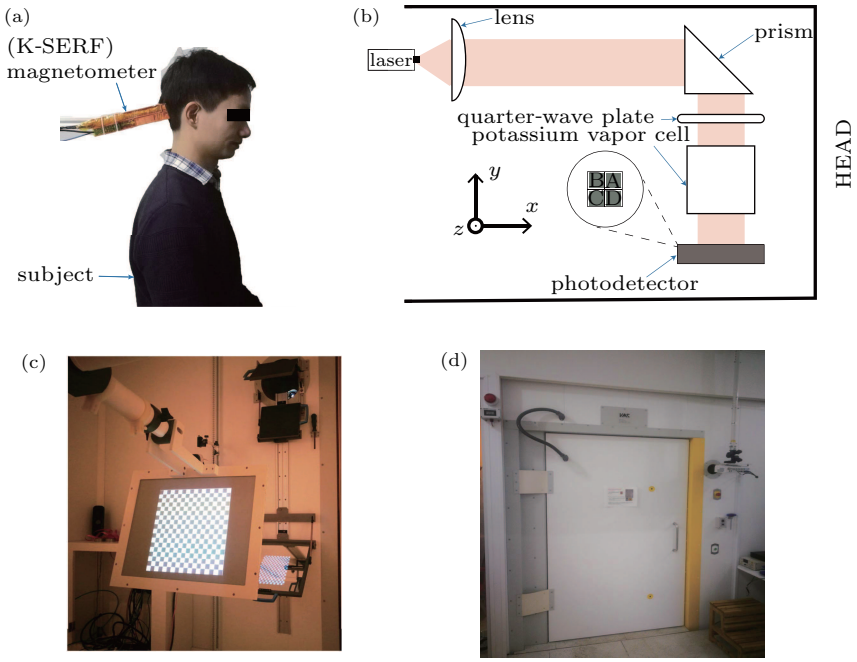


Fig. 2. Experimental equipment for detecting the SSVEP response. (a) Magnetometer is placed at the human head; (b) schematic technical drawing of the compact quad-channel SERF magnetometer; (c) black and white grid for visual stimulation; (d) magnetically shielded room.

The compact quad-channel SERF magnetometer is shown in Fig. 2(a), and its outer dimensions are 20 mm×40 mm×190 mm. Figure 2(b) shows a schematic technical drawing of the OPM. The sensor was operated in a zero-field mode.[28] The microfabricated vapor cell with an internal volume of 8 mm×8 mm×8 mm was filled with naturally abundant potassium, and roughly 1 amagat of N_2 as buffer gas. The vapor cell was heated by electric heaters in order for the K atom vapor to achieve a sufficient density to operate in the SERF[29] regime. The residual magnetic fields in the three directions of the central region of the MSR were about 10 nT (up-down), 15 nT (east-west), and 25 nT (north-south). Three pairs of Helmholtz coils were used to compensate the residual magnetic field around the vapor cell. A 2×2 photodetector array was used to detect the optical signal (shown in Fig. 2(b)). The four elements of the photodetector were named A, B, C, and D, and the area of each element was 4 mm×4 mm. The intrinsic sensitivity of the gradiometer was less than 10 fT/Hz$^{1/2}$. For biomagnetic applications, the sensor should be as close as possible to the scalp to obtain highest possible SNR. In our experiments, the distance between the center of the channel and the scalp was 8 mm for channels A and D, and 12 mm for channels B and C.

3. Experimental results

In our OPM SSVEP recordings, the subject is a healthy adult, without prior training in SSVEP. The optical fiber and wires on the sensor are connected to the external laser and

electronics, respectively, through a small opening in the MSR. The sensor is fixed at the occipital cortex area (see Fig. 2(a)).

The subject is presented with a series of visual stimuli at fixed frequencies. The SSVEP data is collected with a duration of 60 s using the quad-channel OPM, after which the power spectral density (PSD) of the data is calculated. Figure 3 shows the data that come from channel-D in the sensor, for visual stimuli at 10 Hz, 12.5 Hz, and 15 Hz. A clear second harmonic component of these frequencies can be observed in the spectra. The results for other channels follow a similar pattern.

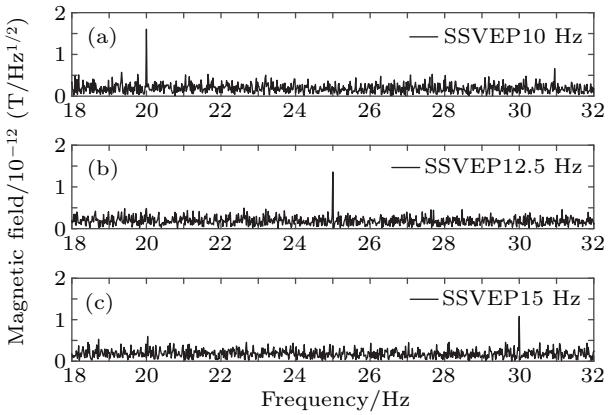


Fig. 3. The PSD of the output signal from channel-D of the OPM sensor at different visual stimuli frequencies: (a) 10 Hz, (b) 12.5 Hz, and (c) 15 Hz.

The signal strength and SNR are two important performance indicators when detecting SSVEPs. The magnetic field from the SSVEP response is measured for 30 s. For each condition, there are seven moving 30-s windows, translated in 5-s steps with respect to one another and covering a total time of 60 s. Figure 4(a) illustrates the measured field strength in response to three stimulation frequencies: 10 Hz, 12.5 Hz, and 15 Hz, with different colors indicating different sensor channels. Figure 4(b) shows the corresponding SNR. As evident from Fig. 4(a), all four quadrants can successfully obtain the SSVEP response, and their signal strengths are in the range of 150 fT–300 fT. We have calculated the SNR, similar to Zhang and colleagues,[30] by dividing the amplitude of the response frequency by the baseline of 2 Hz around that frequency. The SNRs of the four channels at different frequency responses are shown in Fig. 4(b). Depending on the stimulation frequency, the SNRs of the four channels are between 3.5 and 5.5. The response of our OPM has been compared to an EEG device (CTF-275, CTF, Canada) and the signal has been acquired in the same area as for the OPMs. Figure 4(a) shows that the frequency response of our OPM is highly similar to the one from EEG. We can see that the signal strength follows the same pattern for both modalities. Figure 4(b) presents the SNR results. Although EEG shows a higher SNR, its variability is also considerably higher. This may be due to the fact that electric currents underlie the volume conduction, and thus the sources are effectively spread over a larger area. Unlike MEG, EEG requires the use of liquid gel as a conductive medium which works for less than an hour. This procedure significantly complicates the preparation work of the experiment and affects the user experience of the EEG equipment.

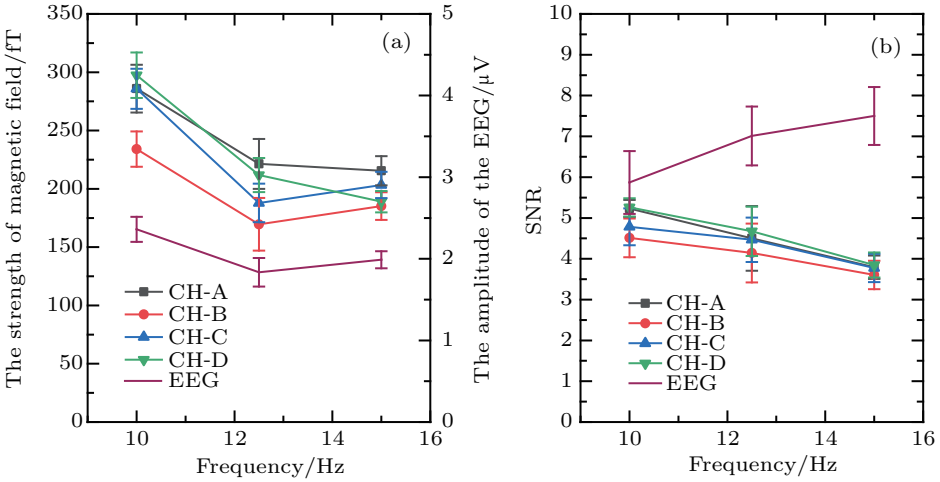


Fig. 4. Colored lines represent the values for the four sensor channels and EEG: CH-A (square), CH-B (circle), CH-C (up triangle), CH-D (down triangle) of the OPM sensor, and EEG (purple line). (a) Magnetic field strength of the SSVEP responses for different stimulation frequencies (10 Hz, 12.5 Hz, and 15 Hz). (b) The SNR for different stimulation frequencies (10 Hz, 12.5 Hz, and 15 Hz).

Gradient measurement[31] is the most efficient way to reduce the environmental noise in MEG by cancelling the common mode noise. Since in our OPMs, four channels are used to observe the SSVEP at the same time, it is possible to achieve gradient measurements with only a single sensor. The time domain signals of channel-A and channel-D are subtracted to form a gradiometer. To test this approach, the subject was presented with visual stimuli at one fixed frequency of 12.5 Hz for 60 s. The PSD of a single channel and a gradiometer were calculated separately. Figure 5 shows that the SSVEP responses can be clearly obtained for a single channel. However, due to short channel separation distance, no significant SSVEP signals can be found using the gradiometer. The occipital region, which processes visual stimuli in the brain, is

larger than the gradient distance (4 mm) of the gradiometer. It appears that during channel subtraction, a substantial amount of SSVEP signal (which is still strong at the farther channel) is removed from the closer channel, thus greatly diminishing the expected gradiometer signal. On the other hand, our set-up is able to suppress the ambient noise by nearly an order of magnitude. In addition to gradient measurements for the SSVEP, the installation of another magnetometer as a reference sensor at a distance of a few centimeters away from magnetic signals from the brain can further reduce the interference of the uniform interference field.

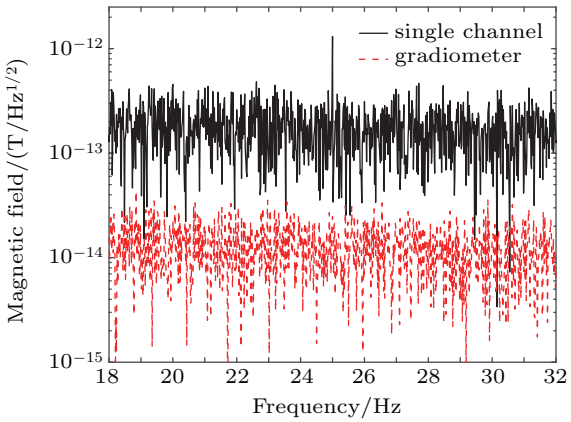


Fig. 5. The response to visual stimuli at a fixed frequency of 12.5 Hz. The PSD of 60 s of SSVEP data for a single channel and gradiometer.

4. Discussion and conclusions

In this study, a self-made quad channel potassium SERF OPM sensor is used to detect the magnetic field of SSVEP signals. Magnetic field intensities ranging from 150 fT to 300 fT are observed for all four channels, and their SNRs lie in the range of 3.5–5.5 with 30-s measurement time. The response of our magnetometer has been compared to an EEG system, showing a similar result. In gradiometer operation, we have achieved significant noise suppression, cancelling the background noise by 20 dB. This gain value has been determined using visual read-out and the following formula: $A(\mathrm{dB}) = 20 \times \log(N_{\mathrm{single}}/N_{\mathrm{gradiometer}}) = 20 \times \log(10^{-13}/10^{-14}) = 20$ dB (Fig. 5), where N is the noise level either for single channel or gradiometer operation. In the case of SSVEP, the channel separation of our sensor is too small relative to the area of the occipital region, resulting in no substantial response from the SSVEP after channel subtraction. Such gradiometer configuration, however, can be useful for many biomedical applications where small magnetic dipole MEG signal is present. MEG systems based on SERF OPM sensors are a highly promising technology in the near future. Further SNR improvements of the SSVEP signal are expected and the bit rate of our approach should soon match that of the current EEG measurements.

References

[1] Hämäläinen M, Hari R, Ilmoniemi R J, Knuutila J and Lounasmaa O V 1993 *Rev. Mod. Phys.* **65** 413
[2] Cohen D 1968 *Science* **161** 784
[3] Detiege X, Lundqvist D, Beniczky S, Seri S and Paetau R 2017 *Seizure* **50** 53
[4] Mouthaan B E, Rados M, Barsi P, *et al.* 2016 *Epilepsia* **57** 770
[5] Bagic A I 2011 *J. Clin. Neurophysiol.* **28** 341
[6] Vantent D, Manshanden I, Ossenblok P, Velis D N, de Munck J C, Verbunt J P A and Lopes da Silva F H 2003 *Clin. Neurophysiol.* **114** 1948
[7] Birbaumer N, Ghanayim N, Hinterberger T, Iversen I, Kotchoubey B, Kübler A, Perelmouter J, Taub E and Flor H 1999 *Nature* **398** 297
[8] Pfurtscheller G, Neuper C, Guger C, Harkam W, Ramoser H, Schlogl A, Obermaier B and Pregenzer M 2000 *IEEE Trans. Rehabil. Eng.* **8** 216
[9] Mullerputz G R, Scherer R, Pfurtscheller G and Rupp R 2005 *Neurosci Lett.* **382** 169
[10] Pfurtscheller G, Müller G R, Pfurtscheller J, Gerner H J and Rupp R 2003 *Neurosci. Lett.* **351** 33
[11] Allison B Z, Wolpaw E W and Wolpaw J R 2007 *Expert Rev. Med. Devices* **4** 463
[12] Mellinger J, Schalk G, Braun C, Preissl H, Rosenstiel W, Birbaumer N and Kübler A 2007 *NeuroImage* **36** 581
[13] Weinstock H 2012 *SQUID Sensors: Fundamentals, Fabrication and Applications* (Chester: Springer Science & Business Media) pp. 491–516
[14] Allred J C, Lyman R N, Kornack T W and Romalis M V 2002 *Phys. Rev. Lett.* **89** 130801
[15] Dang H, Maloof A and Romalis M 2010 *Appl. Phys. Lett.* **97** 151110
[16] Fu J Q, Du P C, Zhou Q and Wang R Q 2016 *Chin. Phys. B* **25** 10302
[17] Li R J, Quan W, Fan W F, Xing L, Wang Z, Zhai Y Y and Fang J C 2017 *Chin. Phys. B* **26** 120702
[18] Sheng D, Perry A R, Krzyzewski S P, Geller S, Kitching J and Knappe S 2017 *Appl. Phys. Lett.* **110** 031106
[19] Alem O, Mhaskar R, Jimenez M R, Sheng D, Leblanc J, Trahms L, Sander T, Kitching J and Knappe S 2017 *Opt. Express* **25** 7849
[20] Knappe S, Alem O, Sheng D and Kitching J 2016 *J. Phys.: Conf. Ser.* **723** 012055
[21] Mhaskar R, Knappe S and Kitching J 2012 *Appl. Phys. Lett.* **101** 241105
[22] Boto E, Holmes N, Leggett J, Roberts G, Shah V, Meyer S S, Munoz L D, Mullinger K J, Tierney T M, Bestmann S, Barnes G R, Bowtell R and Brookes M J 2018 *Nature* **555** 657
[23] Boto E, Bowtell R, Kruger P, Fromhold T M, Morris P G, Meyer S S, Barnes G R and Brookes M J 2016 *PLoS One* **11** e0157655
[24] Xia H, Benamar B A, Hoffman D and Romalis M V 2006 *Appl. Phys. Lett.* **89** 211104
[25] Zhang G, Huang S and Lin Q 2018 *AIP Adv.* **8** 125028
[26] Broser P J, Knappe S, Kajal D S, Noury N, Alem O, Shah V and Braun C 2018 *IEEE Trans. Neural Syst. Rehabil. Eng.* **26** 2226
[27] Beverina F, Palmas G, Silvoni S, Piccione F and Giove S 2003 *PsychNology Journal* **1** 331 ISSN: 17207525
[28] Dupont R J, Haroche S and Cohen T C 1969 *Phys. Lett. A* **28** 638
[29] Happer W and Tang H 1973 *Phys. Rev. Lett.* **31** 273
[30] Zhang S, Han X, Chen X, Wang Y, Gao S and Gao X 2018 *J. Neural. Eng.* **15** 046010
[31] Hansen P, Kringelbach M and Salmelin R 2010 *MEG: an Introduction to Methods* (Oxford: Oxford University Press) pp. 48–49